Available online at www.sciencedirect.com
SCIENCE DIRECT®
Journal of Solid State Chemistry 177 (2004) 126–133
JOURNAL OF SOLID STATE CHEMISTRY
http://elsevier.com/locate/jssc

Energetics of magnesium, strontium, and barium doped lanthanum gallate perovskites

Jihong Cheng and Alexandra Navrotsky*

Department of Chemical Engineering & Material Sciences, Thermochemistry Facility and NEAT ORU, University of California at Davis, 1 Shields Avenue, Davis, CA 95616, USA

Received 10 April 2003; received in revised form 2 June 2003; accepted 6 June 2003

Abstract

$LaGaO_3$ perovskites doped with Sr or Ba at the La site and Mg at the Ga site were prepared by solid-state reaction or sol–gel method and characterized. Enthalpies of formation from constituent oxides at 298 K were determined by high-temperature oxide melt solution calorimetry. Energetic trends are discussed in terms of defect chemistry. As oxygen deficiency increases, formation enthalpies define three trends, $LaGa_{1-y}Mg_yO_{3-\delta}$ (LGM), $La_{1-x}Sr_xGa_{1-y}Mg_yO_{3-\delta}$ (LSGM), and $La_{1-x}Ba_xGa_{1-y}Mg_yO_{3-\delta}$ (LBGM). They become less exothermic with increasing doping, suggesting a dominant destabilization effect from oxygen vacancies. The endothermic enthalpy of vacancy formation is 275 ± 37, 166 ± 18 and 138 ± 12 kJ/mol of $V_O^{\cdot\cdot}$ for LGM, LBGM and LSGM, respectively. Tolerance factor and ion size mismatch also affect enthalpies. In terms of energetics, Sr is the best dopant for the La site and Mg for the Ga site, supporting earlier studies, including oxygen ion conductivity and computer modeling.

Keywords: Enthalpy of formation; Doped lanthanum gallate; Perovskites; Oxygen vacancies; Tolerance factor; Solid oxide fuel cells; Thermodynamics; Solid electrolyte

1. Introduction

There are growing needs for more efficient and environmentally friendly means of energy conversion, among which high-temperature solid oxide fuel cells (SOFCs) are major candidates. Currently, commercial SOFCs utilize yttria-stabilized zirconia (YSZ) as the solid electrolyte operating at about 1273 K [1]. In order to reduce the operating temperature, there are ongoing efforts to identify alternatives for YSZ to make an intermediate temperature SOFC (IT-SOFC).

Sr- and Mg-doped $LaGaO_3$ ($La_{1-x}Sr_xGa_{1-y}Mg_yO_{3-\delta}$, LSGM) was recently proposed as one of the most promising electrolyte candidates for IT-SOFCs because of its high and exclusive oxygen ionic conductivity at 973–1073 K and excellent stability over a broad range of oxygen partial pressure from 1 to 10^{-22} atm [2–5]. Ca- and Mg-doped $LaGaO_3$ (LCGM) and Ba- and Mg-doped $LaGaO_3$ (LBGM) have also been widely investigated as oxygen ion conductors [6–8]. The ionic conductivity of LBGM was reported to be only slightly lower than that of LSGM [6,7] and LCGM was found to be worse than YSZ [6]. The reason for this has not been fully explored though Hayashi et al. [9] have considered structural effects.

In addition to extensive electrical conductivity studies, considerable work has been conducted on mechanical properties [10], thermal expansion [11], crystal structure [12–14] and phase diagrams [5,15,16]. Computer modeling [17] investigated defects and transport properties of doped $LaGaO_3$, predicting that, among alkaline earth cations, Sr and Mg are the most favorable dopants for the La and the Ga sites, respectively.

Little attention has been given to the thermodynamic properties of doped $LaGaO_3$ perovskites. The extent of substitution, the stability under different temperature and oxygen fugacity conditions, and materials compatibility issues all require knowledge of thermodynamic properties. Recently, we presented the enthalpies of formation of $A^{3+}B^{3+}O_3$ perovskites (A = La, B = Al, Ga, Sc and In) which represent parent materials for electrolyte and cathode candidates in SOFCs [18]. Thermodynamic stability was found to decrease (in the

*Corresponding author. Fax: +1-530-752-9307.
E-mail address: anavrotsky@ucdavis.edu (A. Navrotsky).

0022-4596/$ - see front matter © 2003 Elsevier Inc. All rights reserved.
doi:10.1016/S0022-4596(03)00337-2

order Al, Ga, Sc, In) as the tolerance factor deviates more from unity. Doping with alkaline earth cations produces oxygen vacancies which are expected to have profound effects on the thermodynamics.

High-temperature oxide melt solution calorimetry provides a unique tool for studying the energetics of refractory inorganic materials [19,20]. The present work provides reliable thermodynamic data for doped lanthanum gallates. Applicable to SOFCs, this information explores the variation of energetics with structural parameters and anion defects in defect perovskites.

2. Experimental

2.1. Sample preparation

$LaGa_{1-y}Mg_yO_{3-\delta}$ (LGM) and $La_{1-x}Sr_xGa_{1-y}Mg_yO_{3-\delta}$ (LSGM) samples with $0<x$, $y\leqslant 0.20$ were synthesized by conventional solid-state reaction (SSR) from stoichiometric amounts of commercial oxides La_2O_3, Ga_2O_3, MgO and carbonate $SrCO_3$ (purity > 99.99%, La_2O_3 from Aldrich, others from AlfaÆsar). Particular care was paid to La_2O_3 because of its hygroscopic nature [18]. Powders with the proper ratio of required components were mixed thoroughly in an Al_2O_3 mortar and pressed into discs for pre-calcination at 1373 K for 12 h. The heat-treated discs were crushed and ground. The powder resulted were pelletized under a uniaxial pressure of 25 MPa and were sintered at high temperatures (1623–1773 K) in air. All samples were furnace cooled to room temperature. Repeated cycles of grinding, pelletizing and heating on each sample ensured complete reaction. Selected samples were annealed at 1073 K for 3 days and quenched in air.

$La_{1-x}Ba_xGa_{1-y}Mg_yO_{3-\delta}$ (LBGM) samples with $0<x$, $y\leqslant 0.20$ were prepared by a sol–gel method which used acetates, $La(CH_3COO)_3\cdot 1.5H_2O$ (99.99%, AlfaÆsar), $Ba(CH_3COO)_2$ (99.999%, Aldrich) and $Mg(CH_3COO)\cdot 4H_2O$ (99.997%, AlfaÆsar) and nitrate $Ga(NO_3)_3\cdot xH_2O$ (99.9%, AlfaÆsar) as starting materials. The water content of gallium nitrate was determined by thermogravimetry. This nitrate was calcined at 973 K and the weight loss was assigned to the evolution of NO_x and water vapor. The only phase left was Ga_2O_3 after complete decomposition, as confirmed by X-ray diffraction. Three repetitions gave the average value of x as 10.17 ± 0.10.

The sol–gel procedures essentially followed Huang and Goodenough [21]. For each LBGM sample, appropriate amounts of the starting chemicals were dissolved in 200 ml of deionized water with stirring. The clear solution was peptized by adding about 10 ml of aqueous ammonia to form a white gel with pH = 10. The resulting gel was dried in a box oven at 323 K until the loss of NH_3 and H_2O was complete. The dry powder was pre-calcined at 973 K overnight, followed by final sintering at 1673 K for 1 day.

All the sample notations and compositions for single phase materials are given in Table 1. Some other doped $LaGaO_3$ samples (LSGM1005, LSGM1510, LBGM1010 and LBGM1015) were attempted but contained impurities of $SrLaGaO_4$, $SrLaGa_3O_7$, and their Ba analogues. We also attempted to synthesize a series of Ca- and Mg-doped $LaGaO_3$ (LCGM) but neither solid-state reaction nor sol–gel synthesis produced a single phase. Appreciable amounts of $CaLaGaO_4$ and $CaLaGa_3O_7$ were present in every LCGM sample, suggesting extremely small solubility of Ca in $LaGaO_3$.

2.2. Sample characterization

Phase identification was carried out by powder X-ray diffraction (XRD) using a Scintag PAD V diffractometer (Cu$K\alpha$ radiation) operated at 45 kV and 40 mA, with a 0.02 degree step size and 2 s dwell time.

Table 1
Sample notation, composition and structural parameters of LGM, LSGM and LBGM

Sample notation	Nominal composition[a]		Actual composition[a]		Oxygen deficiency δ	Tolerance factor t
	x	y	x	y		
LGM10	0	0.10	0	0.09	0.045	0.962
LGM20	0	0.20	0	0.18	0.090	0.958
LSGM0510	0.05	0.10	0.05	0.10	0.075	0.963
LSGM0515	0.05	0.15	0.05	0.15	0.010	0.960
LSGM1015	0.10	0.15	0.10	0.15	0.125	0.962
LSGM1020	0.10	0.20	0.10	0.20	0.150	0.959
LSGM1520	0.15	0.20	0.15	0.20	0.175	0.961
LSGM2020	0.20	0.20	0.20	0.19	0.195	0.963
LBGM0515	0.05	0.15	0.04	0.15	0.095	0.962
LBGM0718	0.07	0.18	0.06	0.18	0.120	0.963
LBGM1020	0.10	0.20	0.09	0.19	0.140	0.965

[a] Errors (two standard deviations of the mean) are in the range of 0.005–0.015.

Table 2
Thermochemical cycle for calculation of enthalpy of drop solution for AO (A = Sr or Ba) in $3Na_2O \cdot 4MoO_3$ at 975 K

Reaction	ΔH
ACO_3(xl, 298 K) → AO(sol, 975 K) + CO_2(g, 975 K)[a]	$\Delta H(1) = \Delta H_{DS}(ACO_3)$
CO_2(g, 298 K) → CO_2(g, 975 K)	$\Delta H(2) = \Delta H_{298-975}(CO_2)$[b]
AO(xl, 298 K) + CO_2(g, 298 K) → ACO_3(xl, 298 K)	$\Delta H(3) = \Delta H^{\circ}_{f,ox}(ACO_3)$[c]
AO(xl, 298 K) → AO(sol, 975 K)	$\Delta H(4) = \Delta H_{DS}(AO)$
$\Delta H(4) = \Delta H(1)$—$\Delta H(2)$ + $\Delta H(3)$	

[a] xl = crystalline solid; g = gas; sol = solution.
[b] Heat content of CO_2 from 298 to 975 K, calculated from Robie and Hemingway [22], 32.05 kJ/mol.
[c] Calculated from Robie and Hemingway [22], -233.90 ± 1.81 kJ/mol for $SrCO_3$ and -184.61 ± 3.31 kJ/mol for $BaCO_3$.

Table 3
Thermochemical cycle for calculation of the enthalpies of formation of $La_{1-x}A_xGa_{1-y}Mg_yO_{3-\delta}$ (A = Sr or Ba) at 298 K. For LGM, $x = 0$

Reaction	ΔH
La_2O_3(xl, 298 K) → La_2O_3(sol, 975 K)[a]	$\Delta H(5) = \Delta H_{DS}(La_2O_3)$
Ga_2O_3(xl, 298 K) → Ga_2O_3(sol, 975 K)	$\Delta H(6) = \Delta H_{DS}(Ga_2O_3)$
AO(xl, 298 K) → AO(sol, 975 K)	$\Delta H(4) = \Delta H_{DS}(AO)$
MgO(xl, 298 K) → MgO(sol, 975 K)	$\Delta H(7) = \Delta H_{DS}$(MgO)
$La_{1-x}A_xGa_{1-y}Mg_yO_{3-\delta}$ (xl, 298 K) → $\frac{1}{2}(1-x)La_2O_3$(sol, 975 K)	$\Delta H(8) = \Delta H_{DS}$(LAGM)
+ $\frac{1}{2}(1-y)Ga_2O_3$ (sol, 975 K) + xSrO(sol, 975 K) + yMgO(sol, 975 K)	
$\frac{1}{2}(1-x)La_2O_3$(xl, 298 K) + $\frac{1}{2}(1-y)Ga_2O_3$ (xl, 298 K) + xAO(xl, 298 K)	$\Delta H(9) = \Delta H^{\circ}_{f,ox}$(LAGM)
+ yMgO(xl, 975 K) → $La_{1-x}A_xGa_{1-y}Mg_yO_{3-\delta}$ (xl, 298 K)	
$\Delta H(9) = \frac{1}{2}(1-x)\ \Delta H(5) + \frac{1}{2}(1-y)\ \Delta H(6) + x\Delta H(4) + y\Delta H(7) - \Delta H(8)$	

[a] xl = crystalline solid; sol = solution.

A Cameca SX-50 electron microprobe was used for chemical analysis. Sample homogeneity was examined qualitatively by X-ray dot mapping and back-scattered electron images, while quantitative chemical analysis was determined by wavelength-dispersive spectroscopy (WDS). $LaPO_4$, GaAs, $BaTiSi_3O_9$ $SrTiO_3$ and $MgAl_2O_4$ were used as standards for La, Ga, Ba, Sr and Mg, respectively.

Differential scanning calorimetry (DSC) coupled with thermogravimetric analysis (TG) was performed on a Netzsch STA 449 at 298–1273 K. About 50 mg of sample was pelletized to ensure good thermal contact with the Pt crucible and was heated at 10 K/min in an Ar atmosphere with a flow rate of 40 ml/min. Analyses were conducted using the software supplied by the manufacturer after continuous runs of the baseline and sample.

2.3. High-temperature oxide melt solution calorimetry

High-temperature calorimetric measurements were performed in a Tian-Calvet twin microcalorimeter using sodium molybdate ($3Na_2O \cdot 4MoO_3$) as the solvent at 975 K. The equipment and experimental procedures have been described previously [19,20]. Calibration of the calorimeter was based on the known heat content of ~5 mg corundum pellets as a standard laboratory protocol.

A sample pellet weighing ~5 mg was dropped from room temperature into the molten solvent in the calorimeter. The resulting heat effect represents the enthalpy of drop solution (H_{DS}) and is equal to the heat content of the sample from 298 to 975 K plus the heat of solution at 975 K.

Oxygen was flushed through the calorimeter assembly (40 ml/min) to blow out any gas species evolved in the calorimeter. The molten solvent was agitated by bubbling oxygen gas through it (5 ml/min) to facilitate dissolution and prevent local saturation. O_2 was used to assure an oxidizing environment.

SrO and BaO are too hygroscopic to be prepared and handled easily. Their enthalpies of drop solution were calculated from the enthalpies of drop solution of $SrCO_3$ and $BaCO_3$ and other related thermodynamic data using the thermochemical cycle in Table 2. The enthalpies of formation from oxides for the perovskite samples LGM, LSGM and LBGM were calculated using the thermochemical cycle in Table 3.

3. Results and discussion

3.1. Sample characterization

The 11 doped $LaGaO_3$ perovskites were confirmed to be single phases with orthorhombic structure at ambient temperature by powder XRD and to be homogeneous by electron microprobe analysis. The actual compositions of each sample by chemical analysis are listed in Table 1. No phase transitions were observed from DSC of selected samples (LGM20, LSGM2020 and

LBGM0515) at 298–1273 K, indicating either an undetectably small heat of any phase transition ($< \sim 0.05$ kJ/mol) or the stabilization of the orthorhombic structure by doping in this temperature range. A total weight loss of about 0.1 wt% at 350–450 K for each sample was assigned to desorption of a small amount of surface water.

Though it is clear that undoped $LaGaO_3$ is orthorhombic at room temperature and undergoes a phase transition to rhombohedral at 420 K [18,23], discrepancies exist about the structure of Sr- and Mg-doped $LaGaO_3$. For instance, LSGM1020 has been reported to be monoclinic [12], orthorhombic [2,4] or cubic [3,5]. Samples may be different from study to study in synthesis method, sintering conditions, microstructure and ordering state. A detailed neutron diffraction study of our samples is in progress.

3.2. Enthalpies of formation from oxides

The composition of each sample determined by microprobe, rather than the nominal composition, was used in the calculation of enthalpies of formation from oxides. The enthalpies of drop solution of constituent oxides and doped $LaGaO_3$ perovskites and the corresponding enthalpies of formation from oxides at 298 K are summarized in Table 4.

The exothermic enthalpies of formation from oxides show the stability of all 11 perovskites with respect to their component oxides.

3.3. Defect chemistry

Incorporation of alkaline earth cations in $LaGaO_3$, either on the A site or on the B site, will result in at least the following changes:

(1) Oxygen vacancy formation is due to the requirement of charge neutrality after doping. For example, in $La_{1-x}Sr_xGa_{1-y}Mg_yO_{3-\delta}$ (LSGM),

$$SrO + La_{La}^{\times} \rightarrow Sr_{La}' + 0.5V_O^{\bullet\bullet} + O_O^{\times}, \quad (1)$$

$$MgO + Ga_{Ga}^{\times} \rightarrow Mg_{Ga}' + 0.5V_O^{\bullet\bullet} + O_O^{\times}, \quad (2)$$

where Kröger–Vink notation has been adopted [25]. Here the symbol V stands for a vacancy, and the charges are taken relative to the perfect lattice (superscripts $\times$ for neutral, $^{\bullet}$ for positive, and $'$ for negative). The formal concentration of oxygen vacancies can be quantitatively described by the oxygen deficiency, δ, which is equal to $(x + y)/2$ where x and y were determined from chemical analysis (Table 1). The oxygen vacancies may destabilize the system because of the partial disconnection of the corner-shared three dimensional BO_6 octahedral framework [26].

(2) Structure perturbation, either distortion from or recovery toward the cubic structure affects energetics. The tolerance factor, t, describes the relation between symmetry and ionic radii [27]. It is defined as

$$t = \frac{r_{AO}}{\sqrt{2}r_{BO}} = \frac{r_A + r_O}{\sqrt{2}(r_B + r_O)} \quad (3)$$

where r_{AO} and r_{BO} are bond lengths calculated as sums of ionic radii r_A, r_B and r_O. Shannon's radii [28] are adopted for the calculations (see Table 5). Doping modifies this structural parameter considerably. First, the mean ionic radii of A and B sites are calculated as an weighted average, e.g., in a LSGM system:

$$r_A = (1 - x)r_{La^{3+}} + xr_{Sr^{2+}}, \quad (4)$$

$$r_B = (1 - y)r_{Ga^{3+}} + yr_{Mg^{2+}}. \quad (5)$$

Table 4
Enthalpies of drop solution (ΔH_{DS}) of oxides and perovskites in $3Na_2O \cdot 4MoO_3$ at 975 K and enthalpies of formation of perovskites from oxides ($\Delta H^{\circ}_{f,ox}$) at 298 K

Sample	ΔH_{DS} (kJ/mol)	Sample	ΔH_{DS} (kJ/mol)	$\Delta H^{\circ}_{f,ox}$ (kJ/mol)
La_2O_3	-225.10 ± 3.16[a]	LGM10	-24.28 ± 1.66 (11)	-40.37 ± 2.33
Ga_2O_3	106.41 ± 0.88[a]	LGM20	-42.64 ± 2.17 (10)	-27.68 ± 2.71
MgO	-5.79 ± 0.15 (7)[b]	LSGM0510	-25.47 ± 1.32 (10)	-40.94 ± 2.04
$SrCO_3$	130.16 ± 1.66 (10)	LSGM0515	-32.63 ± 0.98 (9)	-36.73 ± 1.84
$BaCO_3$	116.74 ± 1.68[c]	LSGM1015	-35.87 ± 0.55 (9)	-34.65 ± 1.59
SrO	-135.82 ± 2.48[d]	LSGM1020	-41.55 ± 1.46 (12)	-31.92 ± 2.08
BaO	-184.61 ± 3.31[d]	LSGM1520	-47.99 ± 0.86 (12)	-26.64 ± 1.68
		LSGM2020	-49.69 ± 1.10 (11)	-25.52 ± 1.78
		LBGM0515	-36.18 ± 0.29 (7)	-34.90 ± 1.59
		LBGM0718	-42.39 ± 0.63 (8)	-31.90 ± 1.67
		LBGM1020	-47.24 ± 1.02 (7)	-29.80 ± 1.82

[a] From Cheng and Navrotsky [18].
[b] The errors are two standard deviations of the mean. The numbers in ( ) are the number of drops performed.
[c] From Majzlan et al. [24].
[d] From Table 2.

Table 5
Coordination number (CN) and ionic size of the ions in LGM, LSGM and LBGM systems (from Shannon [28])

Site in ABO_3	Ion	CN	Ionic size (Å)
A site	La^{3+}	12	1.40
	Sr^{2+}	12	1.44
	Ba^{2+}	12	1.61
B site	Ga^{3+}	6	0.62
	Mg^{2+}	6	0.72
Oxygen	O^{2-}	6	1.40

The presence of oxygen vacancies will change the coordination number of cations and thus their ionic radii of the cations. However, as a first approximation, the coordination numbers in the ideal perovskite structure are assumed in the calculation of tolerance factor (Tables 1 and 5). The major effect on bond lengths is the ionic substitution on *A* and *B* sublattices. For many perovskites, when *t* deviates slightly from unity, typically in the range of 0.8–1.1, the thermodynamic stability decreases with increasing deviation. This relationship between enthalpy of formation from oxides and tolerance factor has been observed in the system $A^{1+}B^{5+}O_3$ [29], $A^{2+}B^{4+}O_3$ [30,31] and $A^{3+}B^{3+}O_3$ [18].

(3) Ion size mismatch between dopants and host cations on sublattices causes strain and destabilizes the structure.

(4) Oxygen vacancy ordering at low temperatures can affect energetics. Short-range ordering and order–disorder transition phenomena have been studied by neutron diffraction [12,13,32], transmission electron microscopy (TEM) [5,13] and computer modeling [17]. Oxygen vacancies have a strong tendency to be trapped around dopant ions such as Sr_{La}' or Mg_{Ga}' to form vacancy-cation clusters [5,17] that have deleterious effects on the kinetics of oxygen ion migration. In measurements of oxygen ion conductivity of LSGM vs. temperature, the Arrhenius plots exhibited different activation energies in two temperature ranges with a transition at some intermediate temperature [3,5,33]. The higher activation energy in the low-temperature range was attributed to the immobilization effect from short-range vacancy ordering and the transition corresponded to the order–disorder transition.

3.4. Energetic trends

Though the tolerance factor is widely used to systematize the relative stability of perovskite structure, little attention has been paid to the impact of oxygen vacancies, which is a major difference between the previously studied perovskite systems and the doped lanthanum gallates. We thus seek to find regularities in the energetics of these defect perovskites with charge coupled substitution. The effects of oxygen deficiency, tolerance factor and ion size mismatch must be taken into account.

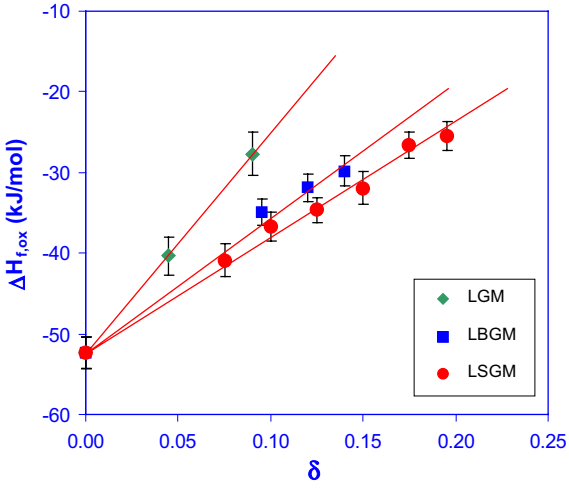

Fig. 1. Enthalpy of formation of doped $LaGaO_3$ from oxides vs. oxygen deficiency.

The enthalpies of formation from oxides for all the 11 doped $LaGaO_3$ samples are plotted vs. the oxygen deficiency in Fig. 1. The data separate into three groups (LGM, LBGM and LSGM). Each group can be fitted as an approximately linear function of oxygen deficiency. These lines intersect at one common point, $\Delta H_{f,ox}$ of undoped $LaGaO_3$, as expected. In all three systems, the enthalpy of formation becomes less exothermic as the oxygen deficiency increases, confirming a destabilizing effect of the vacancy forming substitution on the perovskite structure.

This experimental result is consistent with computer simulations on Sr- and Mg-doped $LaGaO_3$ [11,17]. Khan et al. [17] studied the solution energies of alkaline earth ions in $LaGaO_3$ parent lattices, using the static lattice simulation method in which a shell model was employed instead of the rigid hard-sphere model to incorporate the polarization effect of charged point defects. The solution energies were endothermic. Hayashi et al. [11] used molecular dynamics (MD) simulation to calculate the enthalpies of formation from gaseous ions for a series of LSGM perovskites and found the enthalpy of formation becomes less exothermic with increasing oxygen deficiency.

The slope of each fitted line represents the enthalpy of formation from end members normalized per mole oxygen vacancy and represents the enthalpy of charge coupled substitution. For brevity, we use the short term "enthalpy of vacancy formation" for this slope. The endothermic enthalpies of vacancy formation are 275 ± 37, 166 ± 18 and 138 ± 12 kJ/mol of $V_O^{\bullet\bullet}$ for LGM, LBGM and LSGM, respectively. The enthalpy of vacancy formation in LGM is much larger than that

in LBGM and LSGM while that in LSGM is the least unfavorable.

Since the ionic radius of magnesium is bigger than that of gallium (Table 5), doping of Mg at the Ga site enlarges the average *B*–O bond length, decreasing the tolerance factor. Bearing in mind that the structure of a given group of perovskites becomes less stable as tolerance factor deviates from unity, a smaller tolerance factor corresponds to a less exothermic enthalpy of formation. Therefore, dual effects from the presence of oxygen vacancies and decreased tolerance factor account for the largest destabilization in the LGM system.

The dopant on the *A* site, either Ba or Sr, is bigger than the host La (Table 5), so doping on the La site enlarges the average *A*–O bond length and increases the tolerance factor. Though the role of oxygen vacancy formation is still dominant, the more favorable tolerance factor does explain the much less endothermic enthalpy of vacancy formation in LSGM and LBGM than in LGM. This competition between oxygen vacancy formation and the geometric factor appears similar to that seen in another doped perovskite system, i.e., $NaTi_xNb_{1-x}O_{3-0.5x}$ [34].

The dominant effect of oxygen vacancies on the energetics of doped perovskites can be seen more clearly in Fig. 2 which presents the enthalpy of formation from oxides of selected doped $LaGaO_3$ perovskites vs. tolerance factor. The enthalpies of formation of LGM, LBGM or LSGM are obviously off, in the endothermic direction, the general trend of $A^{3+}B^{3+}O_3$ systems which characterizes vacancy free perovskites.

Doping on the *A* site by a bigger cation will result in the release of the compressive stress on neighboring *B*–O–*B* bonds (*B* = Ga or Mg). The much larger ionic radius of barium than strontium means a larger size mismatch between the dopant and host and thus higher strain energy in LBGM, which probably contributes to larger destabilization than in LSGM.

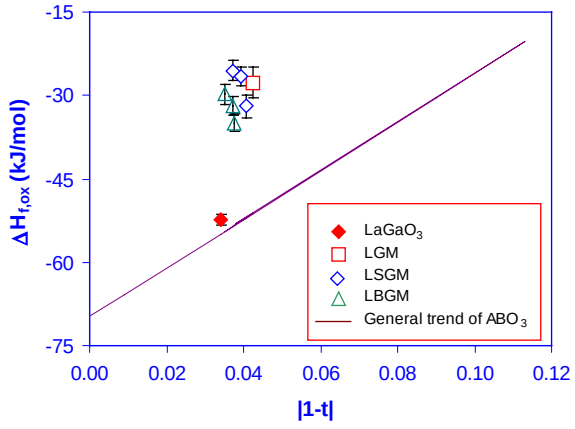

Fig. 2. Enthalpy of formation of doped $LaGaO_3$ from oxides vs. the absolute value of (1–*t*). The linear general trend and the enthalpy of formation of $LaGaO_3$ from oxides were taken from Ref. [18].

Therefore, from the point of view of energetics, Sr is the best substituent on the *A* site and Mg is the best on the *B* site for $LaGaO_3$. This agrees with the atomistic simulation results [17] and is consistent with the electrical property studies which show that simultaneous substitution of Sr and Mg gives the highest ionic conductivity [2,6,9].

3.5. Oxygen vacancy order–disorder

DSC experiments of selected perovskites (LGM20, LSGM2020 and LBGM0515) show no peaks at 773–1273 K, implying either a sluggish vacancy order–disorder transition or a very small heat of transition ($< \sim 0.05$ kJ/mol) if the transition is fast. The drop solution calorimetry experiments show no energetic difference, within experimental error of ~ 1.0 kJ/mol, between the quenched and furnace-cooled samples, which indicates that either the disordering is unquenchable or the enthalpy of any order–disorder transition lies within the accuracy of the high-temperature solution calorimetry. For example, the enthalpy of drop solution of LSGM1020 is -50.05 ± 1.92 kJ/mol for the furnace cooled sample and -49.27 ± 0.86 kJ/mol for the quenched one. The combination of DSC and drop solution calorimetry leads to the tentative conclusion that, whether or not the disordering is quenchable, the order–disorder transition enthalpy is less than 1.0 kJ/mol.

Interestingly, the oxygen vacancies in fluorite-based electrolyte materials, such as yttria stabilized zirconia (YSZ), seem to play a significantly different role in energetics than in doped $LaGaO_3$ perovskites. When C-type Y_2O_3 is introduced into monoclinic ZrO_2, cubic YSZ can be stabilized with anion defect formation:

$$Y_2O_3 + 2Zr_{Zr}^{\times} \rightarrow 2Y_{Zr}' + V_O^{\bullet\bullet} + 3O_O^{\times}. \quad (6)$$

The vacancies are generated by the charge compensation analogous to that in the doped $LaGaO_3$ samples. The enthalpy of charge couple substitution with vacancy formation, which has the same meaning as in this work, is remarkably exothermic, e.g., -105.0 ± 7.2 and -91.4 ± 7.2 kJ/mol of $V_O^{\bullet\bullet}$ for YSZ and calcia-stabilized zirconia (CSZ), respectively [35]. Thus oxygen vacancies stabilize the doped ZrO_2 system, while they dramatically destabilize doped $LaGaO_3$.

Lee et al. [36] recently studied the cubic YSZ solid solution system by oxide melt solution calorimetry and proposed that the presence of substantial short-range order of oxygen vacancies and in cations contributes significantly to the energetic stabilization. Similar stabilization effects are also observed in zirconium oxynitride systems with an even more exothermic enthalpy of vacancy formation, probably because of the higher tendency for long-range ordering than in YSZ and CSZ [37].

The results for YSZ suggest that short-range order dominates the energetics, while the results for doped $LaGaO_3$ suggest a competition between energetically unfavorable vacancy formation and bond length mismatch. A major difference between the perovskite and the fluorite structure is the following. In the perovskite, each oxygen participates in bonding to both *A* and *B* cations, thus the removal of any oxygen perturbs the environment of two *B* cations at the shortest distance and of four *A* cations somewhat further away. Though rotation of the octahedra and relaxation around the oxygen vacancy can mitigate the unfavorable energetics, vacancy formation remains energetically destabilizing. In the fluorite structure, where alternating oxygen cube centers are occupied by cations, the removal of one oxygen perturbs primarily one cation–oxygen bond. Inasmuch as Zr readily accepts both 7- and 8-fold coordination, charge balanced vacancy formation, with enough short-range order so few cubes contain more than one vacancy, appears to be stabilizing. Thus the difference in energetic behavior of the two classes of solid electrolyte materials is understandable in terms of the polyhedral linkages.

4. Conclusions

High-temperature oxide melt solution calorimetry was performed to determine the enthalpies of formation from oxides at 298 K for three groups of doped $LaGaO_3$ perovskites, LGM, LSGM and LBGM. While the presence of oxygen vacancies dramatically destabilizes all three systems due to the breakup of the corner-linked BO_6 framework, other structural parameters such as tolerance factor and ion size mismatch also modify the energetics. The enthalpies of formation from oxides have an approximately linear relationship to oxygen deficiency. The enthalpy of charge balanced vacancy formation was estimated as 275 ± 37, 166 ± 18 and 138 ± 12 kJ/mol of $V_O^{\bullet\bullet}$ for LGM, LBGM and LSGM, respectively. Both vacancy formation and decreased tolerance factor contribute to the most pronounced destabilization in the LGM system. In the LSGM and LBGM systems, the destabilizing effect from oxygen vacancies is still dominant but the more favorable tolerance factor decreases the endothermic enthalpy of the charge balanced substitution. The higher strain energy from bigger ion size mismatch in the LBGM system may explain the more endothermic enthalpy of vacancy formation than in LSGM.

Strontium is the best dopant for the La site and magnesium for the Ga site in $LaGaO_3$ from the point of view of energetics. If any oxygen vacancy order–disorder occurs, its enthalpy is small (<1.0 kJ/mol). The destabilization of oxygen vacancies in these perovskite systems differs from the behavior of the doped ZrO_2 systems in which vacancy forming substitution stabilizes the system by extensive short-range order.

Acknowledgments

The authors thank S. Roeske for the help with the electron microprobe analysis. This project was supported by the U.S. Department of Energy (DOE) (Grant DEFG03-97ER45654).

References

[1] N.Q. Minh, J. Am. Ceram. Soc. 76 (1993) 363.
[2] T. Ishihara, H. Matsuda, Y. Takita, J. Am. Chem. Soc. 116 (1994) 3801.
[3] M. Feng, J.B. Goodenough, Eur. J. Solid State Inorg. Chem. T31 (1994) 663.
[4] P. Huang, A. Petric, J. Electrochem. Soc. 143 (1996) 1644.
[5] K. Huang, R.S. Tichy, J.B. Goodenough, J. Am. Ceram. Soc. 81 (1998) 2565.
[6] J.W. Stevenson, T.R. Armstrong, L.R. Pederson, J. Li, C.A. Lewinsohn, S. Baskaran, Solid State Ionics 113–115 (1998) 571.
[7] S.M. Choi, K.T. Lee, S. Kim, M.C. Chun, H.L. Lee, Solid State Ionics 131 (2000) 221.
[8] S. Kim, M.C. Chun, K.T. Lee, H.L. Lee, J. Power Sources 93 (2001) 279.
[9] H. Hayashi, H. Inaba, M. Matsuyama, N.G. Lan, M. Dokiya, H. Tagawa, Solid State Ionics 122 (1999) 1.
[10] J. Wolfenstine, P. Huang, A. Petric, Solid State Ionics 118 (1999) 257.
[11] H. Hayashi, M. Suzuki, H. Inaba, Solid State Ionics. 128 (2000) 131.
[12] P.R. Slater, J.T.S. Irvine, T. Ishihara, Y. Takita, J. Solid State Chem. 139 (1998) 135.
[13] A. Skowron, P. Huang, A. Petric, J. Solid State Chem. 143 (1999) 202.
[14] N.M. Sammes, G.A. Tompsett, R.J. Phillips, A.M. Cartner, Solid State Ionics. 111 (1998) 1.
[15] S. Kim, K.T. Lee, H.L. Lee, Mater. Lett. 52 (2002) 342.
[16] P. Majewski, M. Rozumek, F. Aldinger, J. Alloys Compd. 329 (2001) 253.
[17] M.S. Khan, M.S. Islam, D.R. Bates, J. Phys. Chem. B 102 (1998) 3099.
[18] J. Cheng, A. Navrotsky, J. Mater. Res., (2003), submitted to.
[19] A. Navrotsky, Phys. Chem. Miner. 2 (1977) 89.
[20] A. Navrotsky, Phys. Chem. Miner. 24 (1997) 222.
[21] K. Huang, J.B. Goodenough, J. Solid State Chem. 136 (1998) 274.
[22] R.A. Robie, B.S. Hemingway, Thermodynamic properties of minerals and related substances at 298.15 K and 1 Bar (10^5 Pascals) pressure and at higher temperatures, U.S. Geological Survey Bulletin, Vol. 2131, Washington, DC, 1995.
[23] W. Marti, P. Fischer, F. Altorfer, H.J. Scheel, M. Tadin, J. Phys. : Condens. Matter 6 (1994) 127.
[24] J. Majzlan, A. Navrotsky, J.M. Neil, Geochim. Cosmochim. Acta 66 (2002) 1839.
[25] F.A. Kröger, H.S. Vink, in: F. Seitz, D. Turnbull (Eds.), Solid State Physics, Vol. 3, Academic Press, New York, 1956, p. 307.
[26] H. Xu, A. Navrotsky, M. Lou Balmer, Y. Su, Mat. Res. Soc. Symp. Proc. 718 (2002) 65.
[27] V.M. Goldschmidt, T. Barth, G. Lunde, W. Zachariasen, Skrifter Norske Videnskaps-Akad. Oslo, I. Mat.-Nat. Kl. 2 (1926) 117.
[28] R.D. Shannon, Acta Crystallogr. A32 (1976) 751.

[29] H. Yokokawa, T. Kawada, M. Dokiya, J. Am. Ceram. Soc. 72 (1989) 152.
[30] A. Navrotsky, Physics and Chemistry of Earth Materials, Cambridge University Press, Cambridge, 1994, p. 243.
[31] S. Ushakov, J. Cheng, A. Navrotsky, J.R. Wu, S.M. Haile, Mat. Res. Soc. Symp. Proc. 718 (2002) 71.
[32] M. Lerch, H. Boysen, T. Hansen, J. Phys. Chem. Solid 62 (2001) 445.
[33] S. Zha, C. Xia, X. Fang, H. Wang, D. Peng, G. Meng, Ceram. Int. 27 (2001) 649.
[34] H. Xu, Y. Su, M. Lou Balmer, A. Navrotsky, Chem. Mater., in press.
[35] I. Molodetsky, Ph.D Thesis, Princeton University, 1999.
[36] T.A. Lee, A. Navrotsky, I. Molodetsky, J. Mater. Res., in press.
[37] I. Molodetsky, A. Navrotsky, F. DiSalvo, M. Lerch, J. Mater. Res. 15 (2000) 2558.